JOURNAL OF CATALYSIS 95, 155–166 (1985)

Hydrogenation of Aromatic Compounds in Synthetic Crude Distillates Catalyzed by Sulfided Ni–W/γ-Al_2O_3

M. F. WILSON, I. P. FISHER,* AND J. F. KRIZ

*CANMET, Energy Research Laboratories, Energy, Mines and Resources Canada, 555 Booth Street, Ottawa, Ontario K1A OG1, and *Gulf Canada Ltd., Research and Development Department, 2489 North Sheridan Way, Sheridan Park, Ontario L5K 1A8, Canada*

Received October 20, 1984; revised March 28, 1985

A presulfided Ni–W/γ-Al_2O_3 catalyst was used to hydrogenate aromatic compounds contained in middle-distillate fractions of Alberta synthetic crudes, in a continuous-flow high-pressure reactor system. The study incorporates detailed compositional analyses of feedstocks and products performed using low-resolution mass spectrometry and ^{13}C NMR. Experimental conditions were such that the effects of thermodynamic equilibria were covered. Differences in reactivity with respect to hydrogenation and cracking were observed for various aromatic species. These allowed comparison of the reaction kinetics and discussion of some mechanistic aspects of catalytic hydrogenation for complex mixtures of hydrocarbons which are not revealed by model compound studies.

INTRODUCTION

The growing trend for substitution of conventional petroleum supplies with synthetic crudes from heavy oils, oil sands and coal, is expected to produce feedstocks low in paraffins and of high aromatic content. The imbalance of hydrogen in distillates from these unconventional sources may be corrected by additional hydroprocessing involving the saturation of aromatic compounds. Previous investigations identified the high processing severities required to produce good-quality transportation fuels from middle distillates of oil sand-derived synthetic crudes (*1, 2*). The Ni–W/γ-Al_2O_3 catalyst used in the present work was found to provide superior hydrogenation activity when compared with the corresponding molybdenum-based hydrotreating catalysts (*2*). The aromatics conversion was monitored by ^{13}C NMR analyses and provided good correlations with fuel properties for processing purposes.

The present work focuses on detailed analysis of compound types within the reactant and product hydrocarbon mixtures using low-resolution mass spectrometry. The method allows the determination of the extent of hydrogenation and cracking, and the effects of thermodynamic equilibria. The phenomena can thus be resolved for the individual compound types in the mixture and related to catalysis of the whole process.

Studies of the reactivity of aromatic components are usually performed using model compounds. An attempt is made to discuss the present findings in view of those published previously. Because of the coexistence of various aromatic species in the hydrocarbon mixture and their competition for the same catalytic sites, it is felt that the comparisons made in this work have practical advantages over those made by using model compounds.

EXPERIMENTAL

The feedstock used in this study was a middle-distillate fraction from a synthetic crude oil produced by fluid coking of Athabasca bitumen. Table 1 presents properties of the feedstock. A commercial NiO–WO_3/γ-Al_2O_3 catalyst (Katalco Sphericat NT-550), evaluated in a previous study, was used for hydroprocessing the feed (*2*).

0021-9517/85 $3.00

TABLE 1

Properties of Middle Distillate Feedstocks from Athabasca Synthetic Crudes

	Synthetic crude A (fluid coked bitumen)	Synthetic crude B (delayed coked bitumen)
Relative density (15/15°C)	0.862	0.836
Carbon (wt%)	87.2	87.5
Hydrogen (wt%)	11.7	12.5
Sulfur (ppm)	97	550
Nitrogen (ppm)	37	54
Average molecular weight	200	201
% Aromatic carbon by ^{13}C NMR	17.5	14.3
Cetane number (CCR method)	31	35
Distillation (D86)		
Initial bp (°C)	163	142
5%	183	
10%	192	181
20%	210	
50%	251	232
90%	296	283
Final bp	318	333

A detailed description of the bench-scale hydrotreating system was given in an earlier report (*3*). The experimental runs were carried out using 70 g of catalyst in 100 cm^3 of reactor volume. The catalyst was sulfided *in situ* at 380°C and atmospheric pressure by passing a mixture of 10% H_2S in hydrogen over the bed for 2 h. The volume of H_2S passed was equivalent to eight times the amount of sulfur required for the formation of sulfides. The continuous-flow reactor was operated in the up-flow mode, the liquid feed and hydrogen were mixed, passed through a preheater and then over the fixed bed of catalyst. The unit ran for 8 h on oil before the first steady-state sample was taken. Experimental runs were carried out at 340–440°C, liquid space velocities of 0.75–2.00 h^{-1} and a hydrogen flow rate at STP of 530 liters (hydrogen) per liter (feedstock) (3000 scf bbl^{-1}). All runs were performed at 170 atm and the hydrogen gas was vented without recycle. The reactor system was maintained at steady-state conditions for 1 h prior to and 2 h during the period in which product was collected.

Compositional analyses of the feedstock and hydrotreated products were performed by low-resolution mass spectrometry using a modification of the method of Robinson (*4*). The samples were run on a CEC 103 mass spectrometer. The aromatic carbon content was determined by ^{13}C NMR analysis using a Varian XL-200 spectrometer. Sulfur content was analyzed by the Wickbold method and carbon, hydrogen, and nitrogen analysis was carried out using a Perkin–Elmer 240B analyzer.

RESULTS AND DISCUSSION

Hydrocarbon Compositions of Syncrude Middle Distillates

The chemical characteristics of middle distillates from the Athabasca syncrudes are significantly different from those of conventional crudes. This is a consequence of the unique oil sands compositions and the upgrading processes employed. The mass spectrometric method used in this work permits the identification of a number of distinct hydrocarbon group types and the amount of each group type found in a particular distillate product is a function of the feedstock source and processing conditions. Table 2 presents compositional analyses of middle-distillate fractions from two Athabasca syncrudes produced by fluid and delayed coking of bitumen and designated A and B, respectively. The distillates have approximately the same boiling range (properties of distillate from syncrude B are presented in Table 1). The analytical technique effectively distinguishes four saturated hydrocarbon group types (which include paraffins and cycloparaffins classified by degree of ring condensation) as well as a range of aromatic hydrocarbon group types. Table 2 shows that for both syncrude distillate fractions the predominant aromatic species are alkylbenzenes, benzocycloparaffins (tetralins), benzodicycloparaffins, and naphthalenes with concentrations decreasing in that order.

TABLE 2

Compositional Analyses (Mass%) of Middle Distillates from Athabasca Syncrudes before and after Secondary Hydrotreating

	Synthetic Crude A	Product from A	Synthetic Crude B	Product from B
	Fluid coked bitumen with primary hydrotreating	Secondary hydrotreating of distillate from A (this work)	Delayed coked bitumen with primary hydrotreating	Secondary hydrotreating of distillate from B (Ref. (*2*))
Paraffins	15.8	19.5	26.4	27.2
Total cycloparaffins	42.4	79.3	48.9	69.6
Noncondensed monocycloparaffins	20.5	39.2	24.5	32.2
Condensed dicycloparaffins	14.4	28.3	16.8	26.3
Condensed polycycloparaffins	7.5	11.8	7.6	11.1
Total aromatics	41.9	1.3	24.8	3.1
Alkylbenzenes	17.3	—	11.3	0.9
Benzocycloparaffins	12.9	0.5	8.7	1.3
Benzodicycloparaffins	5.2	0.6	2.6	0.6
Naphthalenes	3.5	0.2	1.6	0.3
Naphthocycloparaffins	1.6	—	0.1	—
Fluorenes	1.0	—	0.5	—
Triaromatics	0.4	—	—	—
Cetane number	31	42.5	36	45

Note. Experimental conditions: 380°C, 170 atm, LHSV 0.75.

A comparison of the distillate fractions from syncrudes A and B shows some important differences in their chemical compositions. Syncrude A distillates are significantly lower in paraffins (15.8% compared with 26.4%) and also marginally lower in total cycloparaffins than syncrude B distillates. The total aromatic contents of the two syncrude fractions are also significantly different with distillates from A having 17% more. To some extent this may be attributed to differences in severity of primary refinery hydrotreating. These major differences in chemical composition are reflected in the cetane numbers 31 and 36 for distillates from syncrudes A and B, respectively.

Effects of Thermodynamic Equilibrium and Cracking on Hydrocarbon Compositions

Previous work on upgrading of oil sands distillates dealt with the saturation of aromatic compounds and the effect of thermodynamic equilibrium on aromatics conversion (*2*). It has been well established that the saturation of aromatics to naphthenes involves a chemical equilibrium which is shifted in favor of aromatics with increasing temperature:

$$\text{Aromatic} + n\text{-}H_2 \rightleftharpoons \text{Naphthene} \quad (1)$$

Table 2 includes examples of compositional analyses of products from secondary hydrotreating of middle-distillate fractions of syncrudes A and B carried out under optimum processing conditions (380°C, LHSV 0.75, 170 atm). For syncrude B, experiments were from previous work (*2*). It is seen that almost complete elimination of aromatics is achieved and these results confirm previous analysis by ^{13}C NMR. Table 2 also reveals that under optimum conditions for aromatics saturation the paraffin

concentrations of both products have increased marginally indicating that some cracking has occurred, possibly by ring scission of cycloparaffins.

Figure 1 shows summarized chemical changes for conversion of some of the aromatic group types to their corresponding naphthenes. This work demonstrates that such reactions are potentially controlled by thermodynamic equilibria within a range of operating temperatures. Previously, where ^{13}C NMR was used to monitor the effects of changing experimental conditions on aromatics conversion, plots of aromatic carbon content vs temperature were made, the processing effects were "mapped out" with changing LHSV and optimum operating conditions were established (*2*). Figure 2 presents such a plot for hydrotreating syncrude A distillate in which aromatic carbon content (% C_a) is plotted vertically. Each point on the graph gives a value of the total fraction of aromatic carbons compounded over the many different molecular species present in the product sample. The effects

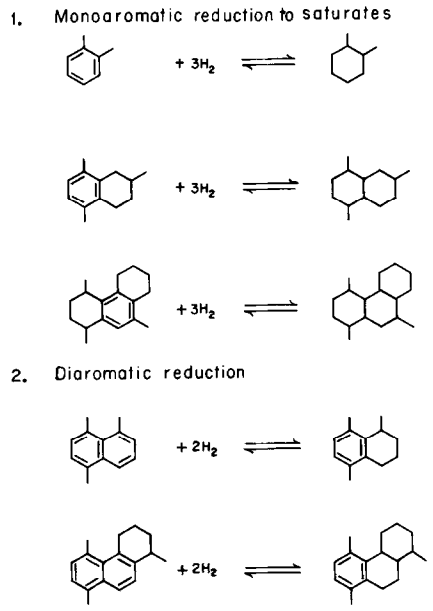

FIG. 1. Summarized chemical changes during hydrotreating of middle distillates from Athabasca syncrudes.

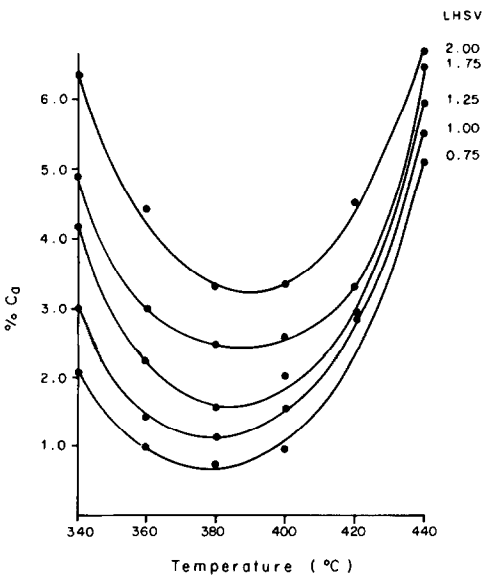

FIG. 2. Effect of LHSV on saturation of aromatics (^{13}C NMR) in syncrude A distillate. Pressure 170 atm.

of temperature and thermodynamic equilibrium are clearly demonstrated as well as the changes in conversion with LHSV. At higher temperatures the curves converge since the equilibrium concentrations are independent of residence time.

An added advantage of using mass spectrometry in the present work is that some of the implicit relationships between the kinetic and thermodynamic equilibrium effects (including cracking) may be resolved by separately mapping out the individual hydrocarbon group types indicated in Fig. 1. Essentially, each point plotted in Fig. 2 is from a different product sample and the corresponding amounts of hydrocarbon group types present as determined by mass spectrometry may therefore be plotted individually. Each of these species may be identified as one of the groups presented in Table 2.

As noted above, the major aromatic hydrocarbon group types are alkylbenzenes, benzocycloparaffins, benzodicycloparaffins, and naphthalenes. Figures 3 to 6 show plots which map out the processing effects for each of these species. The alkylben-

zenes are the largest aromatic hydrocarbon group and their saturation to monocycloparaffins is evident in the lower-temperature range as shown in Fig. 3. A series of smooth, round, almost symmetrical curves is obtained, each with a minimum at 380–400°C. Above this temperature the effect of thermodynamic equilibrium is observed as the concentrations of alkylbenzenes increase again with convergence of curves indicating equilibrium control. In general, the single-ring cycloparaffins are most resistant to cracking (as discussed later with reference to Table 3) and the results indicate that, under these processing conditions, ring-opening is not significant. It therefore appears that the symmetrical shape of curves in Fig. 3 is most representative of a simple reversible reaction unaffected by cracking. In contrast, Fig. 4, which is a similar plot for saturation of benzocycloparaffins to dicycloparaffins, e.g., tetralins to decalins, produces a series of "sharper" curves which show a marked loss of roundness above 380°C. Figure 4 may be linked with Fig. 5 which shows corresponding plots for conversion of benzodicycloparaffins. In this case it is clear that extensive cracking occurs during this reaction above

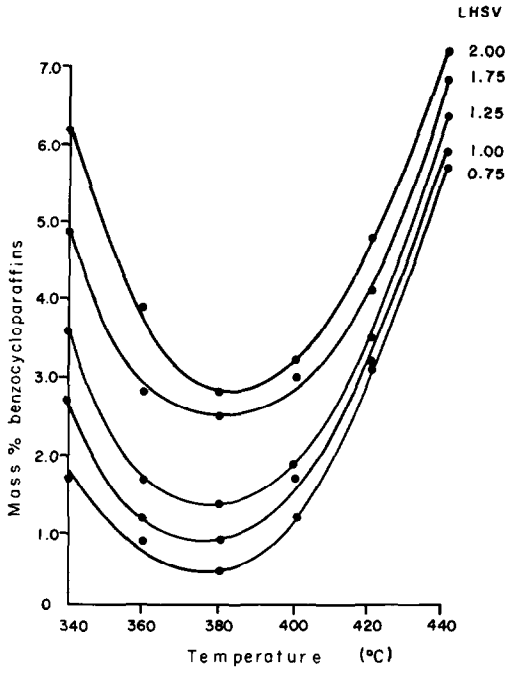

FIG. 4. Effect of LHSV on saturation of benzocycloparaffins in syncrude A distillate. Pressure 170 atm.

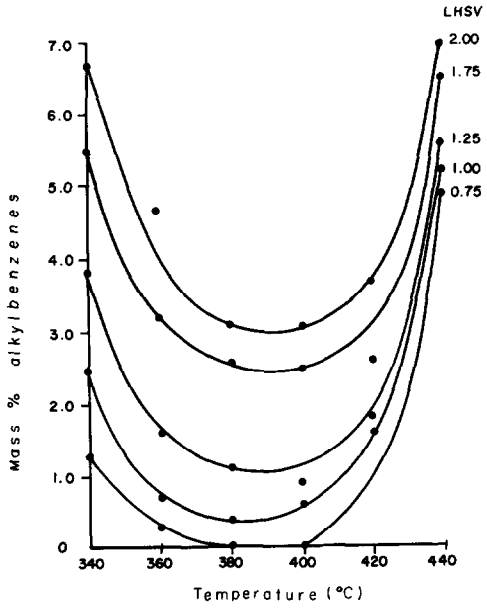

FIG. 3. Effect of LHSV on saturation of alkylbenzenes in syncrude A distillate. Pressure 170 atm.

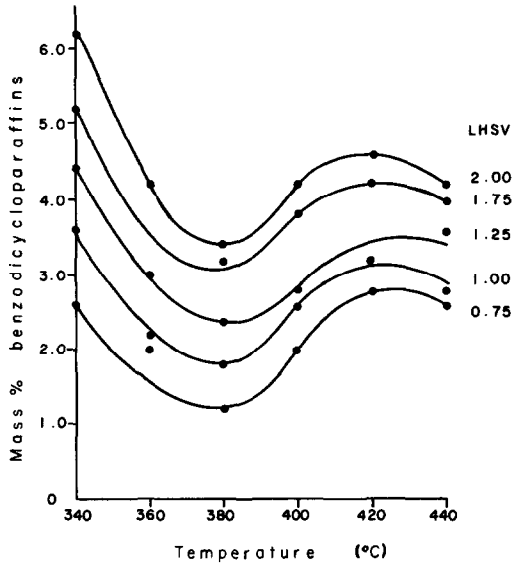

FIG. 5. Saturation and cracking of benzodicycloparaffins in syncrude A distillate. Effects of LHSV at pressure 170 atm.

400°C and the plots pass through a maximum at 420°C and then turn downward, the overall result being a series of s-shaped curves. It is assumed that, in the high-temperature range, ring scission within a condensed three-ring structure occurs with the generation of a corresponding two-ring or single-ring species. Minor distortions of curves in Figs. 3 and 4 may result from these effects. [The s-shape patterns explain similar plots obtained for sulfided Co–Mo/γ-Al_2O_3 catalysts in previous work where ^{13}C NMR analysis was used and where cracking has since been found by mass spectrometry to be very severe (*2*).]

Considering the ease of hydrogenation of various aromatic species, significant differences in reactivity are encountered when comparing the stability of aromatic rings within a series of condensed linearly annulated compounds such as benzene, naphthalene, and anthracene. Lozovoi and Senyavin carried out detailed studies of hydrogenation kinetics of these and other aromatic compounds over WS_2 and MoS_2 catalysts (150–220 atm, 380–475°C) (*5*). On WS_2 these workers found that naphthalene is hydrogenated 23 times and anthracene 62 times faster than benzene. This progression of rates is classically related to a decrease in resonance energy per ring in passing from single-ring through two-ring- to three-ring-condensed linearly annulated compounds. [These results have been confirmed recently by other workers using model compounds and a sulfided Co–Mo/γ-Al_2O_3 catalyst (*6, 7*)]. Also, a comparison of rates for the consecutive hydrogenation reactions of naphthalene to tetralin and tetralin to decalin shows the initial step to be rapid and the final step to be significantly slower. Experimentally, it has been demonstrated that the second reaction is five to eight times slower depending on catalyst type (*5*).

The results obtained for naphthalenes and naphthocycloparaffins hydrogenation in this study are consistent with the above findings. Figure 6 shows a plot of mass% naphthalenes against temperature for a LHSV of 1.00 and 2.00. We find that, in the temperature range of approximately 340–400°C, the naphthalenes-to-tetralins conversion is almost 100%. Similarly, the analysis of product samples for naphthocycloparaffins content gave zero concentrations under all operating conditions. (In the case of naphthalenes a remaining percentage of 0.2 to 0.3% may in fact be an intrinsic analytical error. A small increase in concentration above 400°C can be attributed to the reverse reaction.) Work carried out by Hogan *et al.* (*8*) on hydrogenation of naphthalene and phenanthrene over a sulfided Ni–W/γ-Al_2O_3 catalyst also indicates these phenomena.

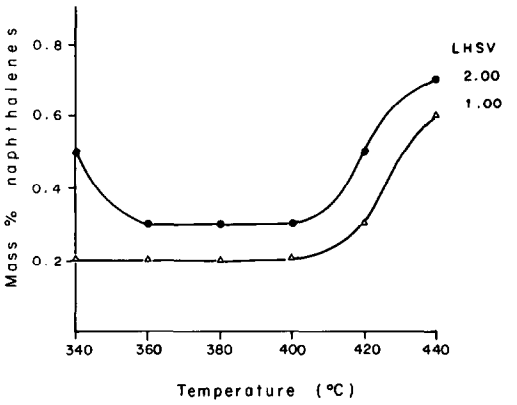

FIG. 6. Conversion of naphthalenes to tetralins in syncrude A distillate. Pressure 170 atm.

The data given in Table 2 show that by mass spectrometry we may also monitor the concentration changes of three cycloparaffinic species with changes in temperature and LHSV. Table 3 presents mass spectrometric data showing the concentrations of monocycloparaffins in the reaction products for each of the given experimental conditions. It shows a matrix of values embracing all combinations of reaction severities. It is observed that the monocycloparaffin concentration generally increases with increase in residence time, temperature, or both. A plot of these results would normally be expected to yield a series of curves with maxima in the range of 380–

TABLE 3

Effect of Temperature and LHSV on Mass % of Monocycloparaffins in Syncrude A Distillate after Secondary Hydrotreating

LHSV	340°C	360°C	380°C	400°C	420°C	440°C
0.75	32.5	33.7	39.2	37.8	38.3	38.7
1.00	31.5	33.8	36.5	34.3	37.0	36.8
1.25	31.2	34.1	34.0	35.7	35.7	33.2
1.75	29.8	33.1	32.8	32.3	32.9	32.7
2.00	28.4	31.7	32.3	32.5	31.9	33.5

400°C, being the inverse of Fig. 3 for the hydrogenation of alkylbenzenes. However, the thermodynamic equilibrium effect is somewhat masked by the effects of cracking of polycyclic naphthenes to monocycloparaffins and is only observed at low residence times. Although the effects are difficult to resolve, the results indicate that cracking of single-ring paraffins is minimal and this is also confirmed by Fig. 3.

The mass spectrometric analyses show that cleavage in two- and three-ring structures occurs under specific processing conditions. Figure 7 presents plots of condensed dicycloparaffins mass% vs temperature and, as expected, the curves produced show an equilibrium effect, and are more or less the mirror image of Fig. 4 (the corresponding plot for benzocycloparaffins). They pass through a maximum at 370–380°C as a result of the equilibrium shift. The plots indicate that, although the dicycloparaffins seem reasonably stable for most of the observed conditions, some cracking is likely at low space velocities, e.g., 0.75, and at higher temperatures (crossing of curves in Fig. 7). Figure 8 is a similar plot for the condensed polycycloparaffins in which case cracking is observed at temperatures as low as 360–380°C.

Under appropriate operating conditions ring-opening reactions may occur at specific catalyst sites in fully or partially saturated aromatic hydrocarbon species. The shift of thermodynamic equilibrium with change in temperature and pressure is also a factor since cracking of aromatic rings may only occur after saturation. A comparison of the results presented in Table 3 and Figs. 7 and 8 for the complete series of cycloparaffins gives some indication of the

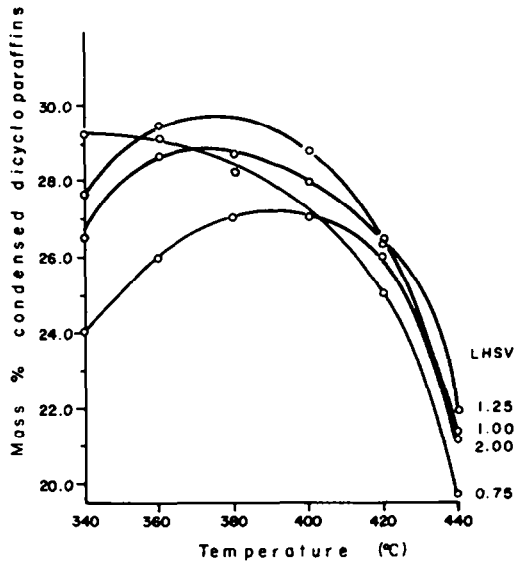

FIG. 7. Formation and dehydrogenation of condensed dicycloparaffins in syncrude A distillate. Effects of LHSV at pressure 170 atm.

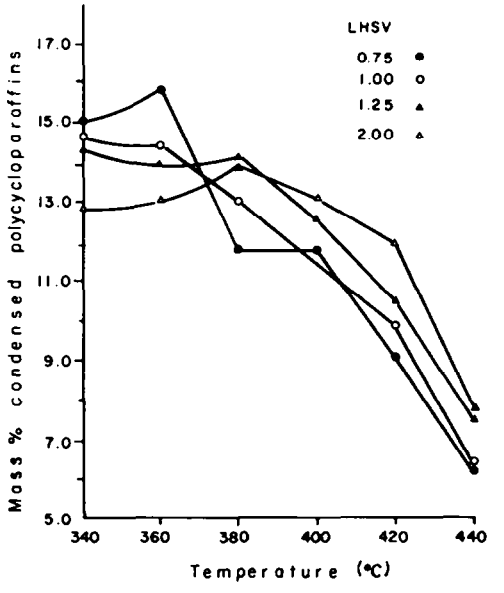

FIG. 8. Dehydrogenation and cracking of condensed polycycloparaffins in syncrude A distillate. Effects of LHSV at pressure 170 atm.

major cracking processes involved. Considering the fully saturated species, it would appear that the order of ease of cracking is three-ring > two-ring > single-ring. Again, there is also strong evidence (considering the results in Table 3 and Fig. 8) that extensive center-ring cracking occurs in three-ring species producing single-ring products.

Kinetics of Aromatic Saturation

The concentration patterns for aromatics and naphthenes show that the temperature range in this study was chosen such that it covers both the kinetic and equilibrium domains. At low temperatures the kinetics control the aromatics conversion whereas at high temperatures the thermodyanic equilibrium has the overriding influence as the reverse reaction becomes increasingly more rapid.

In a previous communication (*2*) the kinetic treatment was based on the simple reversible mechanism of Eq. (1) and the data were fitted into terms resulting from pseudo-first-order reversible kinetics, i.e.,

$$\ln \frac{A - A_e}{A_0 - A_e} = -k_R t, \qquad (2)$$

where A, A_0, and A_e related to product, feed, and equilibrium concentrations of aromatics, respectively, for the reacting mixture, while t and k_R were residence time and rate constant, respectively. The quantity t was calculated from

$$t = \frac{PV_c}{RT} \cdot \frac{1}{\left(\frac{\rho_L}{M_L} + G_L\right) \dot{L}}, \qquad (3)$$

where P, T, V_c, and R are pressure, temperature, catalyst voidage, and gas constant, respectively; while $\dot{L}$, ρ_L, M_L, and G_L are liquid feed flow rate, density, average molecular weight, and hydrogen gas ratio, respectively.

It is felt that the residence time estimated from the above served as a more meaningful quantity in the kinetic analysis than the inverse liquid space velocity. For example, given a particular space velocity, changes in hydrogen flow rates and partial pressures may substantially alter the true contact time. Complete vaporization was assumed and since at high pressures the differences between liquid and gas densities are significantly reduced, the approximation is justified in estimating the residence time. An important simplification incorporated in Eq. (2) is that of a plug-flow regime, although some backmixing can be expected, and thus a more rigorous treatment would have to account for dispersion (*9, 10*). The extent of backmixing was not determined experimentally although a few additional down-flow tests produced results very similar to those of the up-flow arrangement. Since reasonable kinetic plots were obtained by fitting the data in the plug-flow linear-kinetics model, the treatment was considered to be adequate for the purpose of comparisons between the individual aromatic types.

Thus Eq. (2) provided a good interpretation of the observed results and also allowed limited interpretations of the deviations noted. The distortions caused by side reactions prevailing at the higher temperature end were unaccounted for by the kinetic treatment. The cracking reactions were identified as the dominant side reactions to deal with.

The monocyclic hydrocarbons were shown to be most resistant to cracking (Fig. 3), therefore, for these species an attempt was made to predict the equilibrium limitations found by experiment using thermodynamic data from the literature. This provided some estimates of equilibrium constants for the reaction of substituted single-ring compounds of the appropriate carbon number. Only limited thermodynamic data were available but some calculations were possible using data from Stull *et al. (11)*. Stated briefly, effects on the equilibrium by successive substitution of methyl groups into the aromatic ring as well as increasing a single aliphatic side-chain length were examined. It was of interest to find that our experimental data (Fig. 3,

above 420°C) were consistent with these estimates of equilibrium constants, provided that more than one substituent was involved.

The present study, which focuses on resolving the hydrogenation reactions into those of representative hydrocarbon groups, could also use Eq. (2) for the kinetic treatment. As indicated above, this approach would be particularly suitable for the hydrogenation of alkylbenzenes to monocycloparaffins where very little complication was evident in accounting for different reactions. However, the other typical reactions investigated did exhibit such complications at the high-temperature end. To avoid confusion, and yet provide kinetic parameters for comparative purposes, a simplifying assumption of pseudo-first-order irreversible kinetics was made to treat all data provided by mass spectrometry and ^{13}C NMR:

$$\ln \frac{A}{A_0} = -kt, \qquad (4)$$

where k = the rate constant. This approach was proved to be justified, but only within the lower temperature range, where the effect of equilibrium was insignificant in terms of the overall precision. Data evaluations showed that within the temperature range 340–380°C, at 170 atm, Eq. (2) effectively reduces to Eq. (4) without significant loss of precision.

Reaction profiles for saturation of aromatics in syncrude A middle distillate are presented in Fig. 9. These simple plots compare the reaction rates of the major aromatic hydrocarbon group types at 380°C. It is apparent that the naphthalenes are rapidly converted to low concentrations in the initial seconds of reaction and as indicated above the experimental data show that the naphthocycloparaffins are similarly eliminated. (In the case of naphthalenes this is also confirmed by the data in Fig. 6.) For the purpose of making pseudokinetic calculations it was therefore assumed that, under the given experimental conditions, all naph-

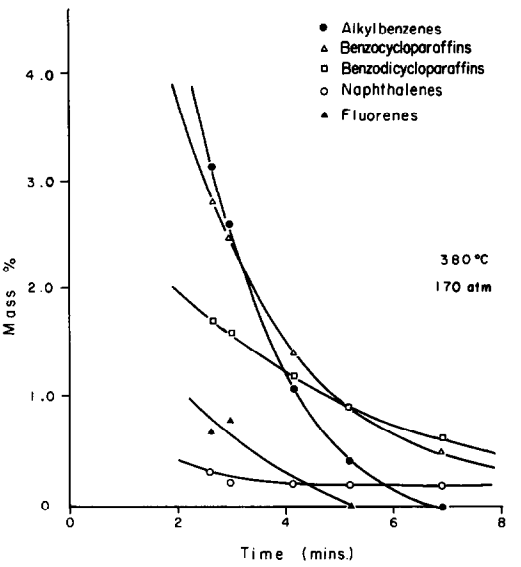

FIG. 9. Reaction profiles for hydrogenation of aromatic group types in syncrude A distillate.

thalenes and naphthocycloparaffins were in their corresponding hydroaromatic forms. (Again, since the concentrations of these species in the feed were low, i.e., 3.5 and 1.6%, respectively, these approximations are good.)

Using mass spectrometric data for syncrude A distillate in the lower temperature range, pseudo-first-order kinetic plots of $\ln(A/A_0)$ vs t were made for saturation of alkylbenzenes, benzocycloparaffins (tetralins), and benzodicycloparaffins. A typical kinetic plot for saturation of alkylbenzenes is presented in Fig. 10. Values of the pseudo-rate-constants, k, for the above species were determined from the kinetic data by regression analysis and are presented in Table 4. Thus the reaction rates for the three hydrocarbon group types may be compared. In each case the reaction involves the saturation of a single aromatic ring in a series of compound types of varying degrees of ring condensation, the resultant products being one-, two-, and three-ring cycloparaffins. (These reactions are represented by the first three examples given in Fig. 1 for monoaromatic reduction to saturates.) It is apparent from Table 4

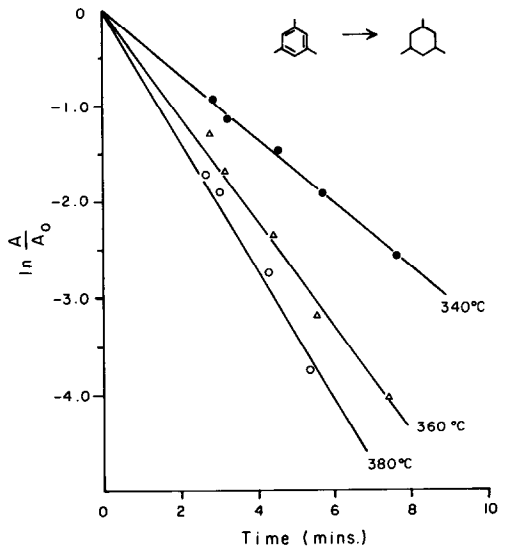

FIG. 10. Pseudo-first-order kinetics for hydrogenation of alkylbenzenes.

that the rate of the reaction decreases in the order alkylbenzenes > benzocycloparaffins > benzodicycloparaffins, i.e., with increase in number of condensed rings per reacting monoaromatic species. Since the saturated rings in these structures are bulky and nonplanar we attribute the decrease in reaction rates to steric effects which hinder the mobility of the reacting species in their competition for catalytic sites. (This is the reverse of the order of rates obtained for linearly annulated aromatic species mentioned above (*5*, *7*).) It is also expected that the rate of saturation of the remaining single aromatic ring in a condensed ring structure will be slow compared with saturation of the preceding rings in that structure because of the effects of resonance energy discussed previously.

For the hydrotreating catalysts (sulfided Co–Mo, Ni–Mo, and Ni–W on γ-Al_2O_3) it is generally believed that the catalytic sites are surface anion vacancies which expose the major metal cation (Mo or W) and thus allow bonding to the aromatic nucleus by interaction with its π electrons (*2*). It is thought possible that the intermediate π-bonded species may rearrange to the corresponding σ-bonded form such that hydrogen addition may occur in a manner resembling electrophilic aromatic substitution (*6*).

Broderick *et al.* (*7*) also claim that these sites will allow bonding of large aromatic molecular species, e.g., benzonaphthothiophene with no evidence of steric hindrance. This points to a "flat" π-bonded structure of the adsorbed species. These authors also speculate that in the sulfided Co–Mo/γ-Al_2O_3 catalyst, adsorption may involve an intercalation such that the flat aromatic molecule is inserted (at the crystal edge) between the parallel layers of sulfur ions in the MoS_2 structure (*7*). The results obtained above for the reaction of a

TABLE 4

Pseudo-Rate-Constants, Activation Energies, and Log Preexponential Factors for Saturation of Aromatic Compounds over Sulfided Ni–W/γ-Al_2O_3

Aromatic type	Pseudo-Rate-Constants (min^{-1})			Activation energy ($kJ\ mol^{-1}$)	ln *A*
	340°C	360°C	380°C		
Alkylbenzenes (syncrude A)	0.33 ± 0.01	0.54 ± 0.05	0.66 ± 0.09	57 ± 13	10.1 ± 2.5
Benzocycloparaffins (syncrude A)	0.31 ± 0.03	0.45 ± 0.10	0.53 ± 0.09	44 ± 9	7.5 ± 1.6
Benzodicycloparaffins (syncrude A)	0.25 ± 0.05	0.34 ± 0.14	0.39 ± 0.09	39 ± 10	6.2 ± 1.9
Aromatic carbon ^{13}C NMR (syncrude A)	0.30 ± 0.06	0.44 ± 0.09	0.50 ± 0.11	44 ± 11	7.5 ± 1.2

series of nonplanar aromatic species over sulfided Ni–W/γ-Al_2O_3 would support the idea of intercalation in view of the evidence for steric hindrance.

For comparison, Table 4 presents corresponding pseudo-first-order rate constants for conversion of the total aromatic carbon content of the feed in the low-temperature range, and uses ^{13}C NMR data presented in Fig. 2. Since the ^{13}C NMR data give only the rate of conversion of the aromatic carbon fraction of the feed without distinguishing different molecular species, we expect some averaging of the rates obtained for the individual hydrocarbon group types.

Values of the pseudo-rate-constants were used to evaluate activation energies by means of the Arrhenius equation

$$\ln k = \ln A - E/RT, \qquad (5)$$

where A = the Arrhenius preexponential factor; E = the activation energy; and R = the gas constant.

Figure 11 presents Arrhenius plots for the alkylbenzenes, benzocycloparaffins, and benzodicycloparaffins in syncrude A distillate as well as the corresponding plot

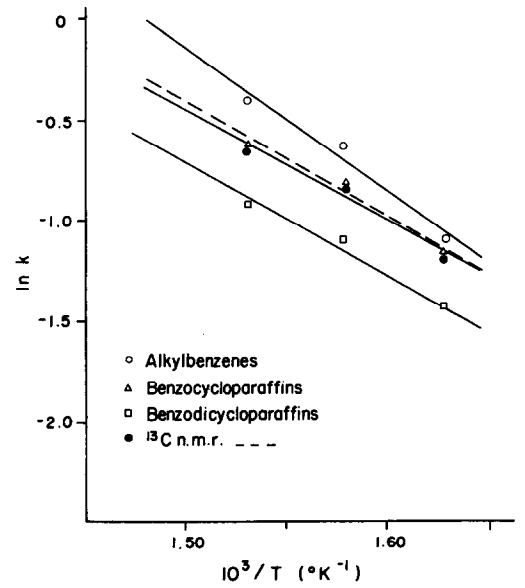

FIG. 11. Arrhenius plot of pseudo-rate-constants for hydrogenation of aromatic group types.

TABLE 5

Arrhenius Parameters for Hydrogenation of Aromatic Hydrocarbons over Sulfided Tungsten–Molybdenum-Based Catalysts

Aromatic type	Activation energy (kJ mol^{-1})	ln A	Reference
Ni–W/γ-Al_2O_3			
Benzene	71	—	Voorhoeve and Stuiver (*12*)
Aromatic carbon ^{13}C NMR (syncrude B)	60 ± 4	10.6 ± 0.8	Wilson and Kriz (*2*)
Ni–Mo/γ-Al_2O_3			
Aromatic carbon ^{13}C NMR (syncrude B)	83 ± 3	14.7 ± 0.5	Wilson and Kriz (*2*)
Co–Mo/γ-Al_2O_3			
Dibenzothiophene	117	—	Broderick and Gates (*13*)
Biphenyl	142	—	Sapre and Gates (*14*)
Aromatic carbon ^{13}C NMR (syncrude B)	63 ± 9	10.5 ± 1.8	Wilson and Kriz (*2*)

for the ^{13}C NMR results. The data gave parameters which are presented in Table 4.

For the monoaromatic hydrocarbon group types, it is apparent that the activation energy of 57 kJ mol^{-1} for saturation of alkylbenzenes is significantly higher than the corresponding values for benzocycloparaffins and benzodicycloparaffins (44 and 39 kJ mol^{-1}, respectively). Within the temperature range studied, the high reactivity of alkylbenzenes is thus accounted for by the preexponential factor, rather than the activation energy. This again indicates that steric hindrance may inhibit the reaction of the two- and three-ring species. Figure 11 also indicates that the Arrhenius plots for alkylbenzenes and benzocycloparaffins would intersect at approximately 320°C at which temperature their reaction rates would be equal. Some comparisons of Arrhenius parameters from the literature are presented in Table 5. For reactions over sulfided Ni–W/γ-Al_2O_3 reasonably good agreement of activation energies is obtained for hydrogenation of alkylbenzenes (this work, Table 4) and the value, 71 kJ mol^{-1}, found by Voorhoeve and Stuiver for benzene at 300–400°C (*12*). From our pre-

vious work using ^{13}C NMR data, hydrogenation of syncrude B distillates over different hydrotreating catalysts (Ni–W, Ni–Mo, Co–Mo) yielded activation energies in the range 60–80 kJ mol^{-1}. Table 5 shows that significantly higher values were obtained by Broderick, Sapre, and Gates for hydrogenation of dibenzothiophene and biphenyl over sulfided Co–Mo/γ-Al_2O_3 (*13, 14*). These results are not readily explainable but may be attributed to differences in aromatic type. Again, we note that in our own work, the ^{13}C NMR data for hydrogenation of distillates from syncrudes A and B over sulfided Ni–W/γ-Al_2O_3 give significantly different values of 44 and 60 kJ mol^{-1}, respectively.

SUMMARY AND CONCLUSIONS

Differences in hydrocarbon composition of middle distillate fractions from two Athabasca syncrudes produced by delayed and fluid bed coking of bitumen have been established. High-pressure hydrotreating of these distillates over sulfided nickel–tungsten has in some cases produced almost complete conversion of aromatics. The differences in reactivity of aromatic and saturate species were used to distinguish various processing phenomena such as the effects of thermodynamic equilibrium and cracking. Distortion of curves previously obtained using ^{13}C NMR analyses alone were thus explained using mass spectrometry. The order of cracking in cycloparaffinic structures is also related to the degree of ring condensation and observed effects range from center-ring cracking in polycyclic structures to minimal ring scission in stable monocyclics.

For saturation of different monoaromatic group types it is shown that the degree of condensation with saturate rings is an important factor in determining ease of hydrogenation. Steric effects appear to influence reaction rate. The enhanced hydrogenation activity of naphthalenes and naphthocycloparaffins over monoaromatics is explained in terms of decreased resonance energy per ring for these species.

Examination of Arrhenius parameters for aromatics saturation suggests that the alkylbenzenes require more activation than other aromatic species but at higher temperatures their conversion is faster due to reduced steric effects. Since all of these catalyzed reactions occur simultaneously in the same reaction mixture, these observations present a practical picture of the various processes involved.

ACKNOWLEDGMENTS

The authors wish to thank M. Stolovitsky for performing hydrotreating experiments, G. de Boer for mass spectrometric analyses, and G. W. Buchanan, Carleton University, Ottawa, for ^{13}C NMR determinations. We also thank the Alberta Research Council, Syncrude Canada Ltd. and Suncor Inc. for providing samples of synthetic crude oil.

REFERENCES

1. Wilson, M. F., CANMET Report 82-2E, "Impact of Excessive Aromatics in Oil Sand Syncrudes on Production and Quality of Middle Distillate Fuels," November 1981.
2. Wilson, M. F., and Kriz, J. F., *Fuel* **63,** 190 (1984).
3. Takematsu, T., and Parsons, B. I., Technical Bulletin TB 187. Department of Energy, Mines and Resources, Ottawa, Canada, 1972.
4. Robinson, C. J., *Anal. Chem.* **43,** 1425 (1971).
5. Weisser, O., and Landa, S., "Sulfide Catalysts: Their Properties and Applications." Pergamon, New York, 1973.
6. Sapre, A. V., and Gates, B. C., *Ind. Eng. Chem. Process Des. Dev.* **20,** 68 (1981).
7. Broderick, D. H., Sapre, A. V., Gates, B. C., Kwart, H., and Schuit, G. C. A., *J. Catal.* **73,** 45 (1982).
8. Hogan, R. J., Mills, K. L., and Lanning, W. C., *Prep. Div. Petrol. Chem. Amer. Chem. Soc.* **5,** B-5 (1960).
9. Carberry, J. J., "Chemical and Catalytic Reaction Engineering." McGraw–Hill, New York, 1976.
10. Levenspiel, O., "Chemical Reaction Engineering." Wiley, New York, 1972.
11. Stull, D. R., Westrum, E. F., and Sinke, G. R., "The Chemical Thermodynamics of Organic Compounds." Wiley, New York, 1969.
12. Voorhoeve, R. J. H., and Stuiver, J. C. M., *J. Catal.* **23,** 228 (1971).
13. Broderick, D. H., and Gates, B. C., *AIChE J.* **27,** 663 (1981).
14. Sapre, A. V., and Gates, B. C., *Ind. Eng. Chem. Process Des. Dev.* **21,** 86 (1982).